




# Evaluation of a novel elastic registration algorithm for spinal imaging data: A pilot clinical study

Ashkan Rashad<sup>1</sup>  | Max Heiland<sup>2</sup> | Patrick Hiepe<sup>3</sup> | Alireza Nasirpour<sup>1</sup> | Carsten Rendenbach<sup>2</sup> | Jens Keuchel<sup>3</sup> | Marc Regier<sup>4</sup> | Ahmed Al-Dam<sup>1</sup>

<sup>1</sup>Department of Oral and Maxillofacial Surgery, University Medical Center Hamburg-Eppendorf, Hamburg, Germany

<sup>2</sup>Department of Oral and Maxillofacial Surgery, Charité—Universitätsmedizin Berlin, Freie Universität Berlin, Humboldt-Universität zu Berlin, and Berlin Institute of Health, Berlin, Germany

<sup>3</sup>Brainlab AG, Munich, Germany

<sup>4</sup>Diagnostic and Interventional Radiology and Nuclear Medicine, University Medical Center Hamburg-Eppendorf, Hamburg, Germany

## Correspondence

Dr. Ashkan Rashad, Department of Oral and Maxillofacial Surgery, University Medical Center Hamburg-Eppendorf, Martinistrasse 52, 20246 Hamburg, Germany.  
Email: a.rashad@uke.de

## Funding information

Brainlab AG

## Abstract

**Background:** Rigid image coregistration is an established technique that allows spatial aligning. However, rigid fusion is prone to deformation of the imaged anatomies. In this work, a novel fully automated elastic image registration method is evaluated.

**Methods:** Cervical CT and MRI data of 10 patients were evaluated. The MRI was acquired with the patient in neutral, flexed, and rotated head position. Vertebrawise rigid fusions were performed to transfer bony landmarks for each vertebra from the CT to the MRI space serving as a reference.

**Results:** Elastic fusion of 3D MRI data showed the highest image registration accuracy (target registration error of 3.26 mm with 95% confidence). Further, an elastic fusion of 2D axial MRI data (<4.75 mm with 95% c.) was more reliable than for 2D sagittal sequences (<6.02 mm with 95% c.).

**Conclusions:** The novel method enables elastic MRI-to-CT image coregistration for cervical indications with changes of the head position.

## KEYWORDS

cervical spine, co-registration accuracy, CT, deformable registration, elastic fusion, image registration, MRI, rigid fusion, spine curvature correction

## 1 | INTRODUCTION

Different medical imaging modalities have been developed so far providing complementary diagnostic or therapeutic information. Combining various imaging modalities facilitates comparison and interpretation of images acquired at different time points, where the patient's anatomy might have been subjected to positional alternations.<sup>1-3</sup> Nowadays, more complex intervention approaches and increased economic pressure have encouraged the need for sophisticated image processing technology.<sup>4</sup>

Image coregistration, introduced about two decades ago, allows the determination of the spatial transformations or mappings in one image that corresponds to the same structure in another image, resulting in the merging of images based on the relations.<sup>5</sup> For instance, image coregistration helps to transfer the surgical plan's

coordinate system to that of the operating room by spatial matching the preoperative and intraoperative images, thereby allowing the surgeon to precisely plan the surgical trajectory while preserving the vulnerable neighboring anatomy.<sup>6</sup> So far, this method has been employed in many medical fields such as neurosurgery, ENT, skull base surgery, and radiotherapy, showing clinical benefit compared with procedures without application of any image coregistration.<sup>7-13</sup>

MRI and CT are the most frequently used modalities to obtain preoperative imaging data for spinal surgeries. While MRI provides high soft tissue contrast, CT allows high-resolution imaging of bony structures.<sup>3</sup> The current standard approach to fuse MRI and CT images is given by linear, rigid image coregistration (or "rigid image fusion"), which allows alignment of images with six degrees of freedom (DOF; translation and rotation along x, y, z directions). Spatial alignment between the fused images is maximized based on the employed



similarity criteria (eg, mutual information or correlation coefficient metrics), enabling a multimodal comparison of superimposed images.<sup>1</sup> This approach, however, requires that imaged anatomies remain unchanged in their spatial dimensions.

Initial efforts on medical imaging were focused on rigid registration of brain images given that scarce change happens in brain position or shape between short periods of data acquisition, where rigid registration could successfully calculate shear and scaling discrepancies in images. The challenge happens where employing this method to organs that lack such rigid structures where images would be subjected to not only global but also local nonrigid deformities. In this case, employing a hybrid registration seems inevitable when translations and rotations have to be corrected by a preliminary registration before correcting nonlinear deformities. Elastic registration could be employed when dealing with patient movement, change of the anatomy over time, or deformities caused by injection of contrast agents. This method corrects local nonlinear deformities using localized image stretching.<sup>14,15</sup> Nonlinear, nonrigid image coregistration techniques account for nonrigid morphological inconsistencies between the different datasets and are based on the determination of a “deformation vector” for each image voxel so that the 3D deformation vector field maximizes the similarity between the fused images.<sup>16</sup> Studies have suggested that elastic image fusion reduces the image registration error in comparison with rigid transformation.<sup>17</sup> Because of the flexibility of the spine, it is potential to movements during the imaging process, limiting the reproducibility of patient positioning and thus the imaging of same anatomies and their spatial relations during multiple sessions.<sup>18,19</sup> As a previous solution, in a study carried out by Klabbers, it was reported that rigid registration of PET-CT with immobilization could reduce the mean translation error.<sup>20</sup> Although this technique might not be applicable in all surgical situations where rigid image registration cannot compensate for complex spatial dynamics.

The aim of the present study is to assess the reliability of a novel, commercially available elastic image coregistration method (Elements Spine Curvature Correction, Brainlab AG, Germany) for cervical MRI-CT image data showing significant positional changes between the scans. The proposed method is designed to compensate for changes of the spine curvature by considering the rigidity of vertebral bodies and the natural flexibility of the intervertebral discs. The image registration accuracy for rigid and elastic image fusion was retrospectively measured by landmark-based quantitative evaluation. It was hypothesized that the proposed method enables elastic image coregistration with registration accuracy in the range of the spatial image resolution, and therefore may represent a reliable tool for cervical spine surgeries.

## 2 | MATERIALS AND METHODS

### 2.1 | Imaging studies

After approval by the local ethics committee (reg no.: PV4928) and receiving the written consent of each patient, CT and MRI data of 10 subjects were retrospectively analyzed in this study. MRI imaging

was performed on patients who have undergone CT imaging of the head and neck region for diagnostic purposes independently of the study. All patients were scanned preoperatively suffering from cancer of the head and neck region. The CT scans were acquired by using a standard clinical CT device (Philips Brilliance 64, Philips, Best, the Netherlands) with the field of view (FOV) adjusted to cover the whole body along the entire cervical spine as well as parts of the superior thoracic spine (depended on the clinical indication). The MRI protocol was conducted on a clinical whole-body 3-T MRI scanner (Philips Ingenia, Philips, Best, the Netherlands) and included 3D T<sub>1</sub>-weighted (T<sub>1</sub>w), 2D axial T<sub>1</sub>w, T<sub>2</sub>w, fat-suppressed, 2D sagittal T<sub>1</sub>w, T<sub>2</sub>w, and fat-suppressed MRI (details are given in Table 1). Repetitive application of this protocol with the patient in neutral, flexed, and rotated head position was carried out in order to induce maximum translational and rotational displacements of cervical and thoracic vertebrae relative to each other. Overall, N = 210 CT-MR fusion pairs were investigated in this study (by evaluating 3 head positions × 7 MRI scans × 10 patients).

### 2.2 | Elastic image fusion

The basic idea of the proposed method (Elements Spine Curvature Correction, Brainlab AG, Germany) is to automatically calculate individual rigid image coregistration for each vertebra and, afterwards, to determine a single 3D deformation field that matches all vertebrae in the fused images at the same time. To this end, the software triggers the automatic image segmentation of the (preoperative) CT scan provided by a synthetic tissue model (US patents US9639938, US9704243), which, thereby, yields the location of the *n* imaged vertebrae in the CT scan.<sup>19</sup> Thereafter, a region of interest (ROI) is defined for each localized vertebra in which a rigid image coregistration between the CT and MR images will be performed using mutual information (MI)-based rigid fusion algorithm.<sup>20</sup>

A starting point for the algorithm serves a manual prealignment of the datasets via the GU of the proposed software (shown in Figure 1, left). This initial rigid registration is subsequently used to find the vertebra that served for the prealignment (by comparing the results of the input rigid fusion with those determined for ROI corresponding to a specific vertebra). The corresponding vertebrae-specific rigid registration is further used to iteratively calculate the rigid fusions of the superiorly and inferiorly neighbored vertebrae, but taking the result of previous ROIs into account (by constraining translational and rotational differences between neighbored vertebrae). The result of this process is *n* vertebra-specific rigid registrations, which are used to determine a 3D deformation field by interpolating between the segmented and rigidly registered vertebrae (Figure 1, right).

### 2.3 | Registration accuracy measurement

In order to assess the image registration accuracy of the proposed method, *n* vertebra-specific prealignments of each MR-CT data pair and, thus, a broad range of vertebrae displacements for different MRI sequences were used to measure the image registration accuracy

**TABLE 1** MRI sequence protocol specifications

Sequence <sup>a</sup>	Acquisition Type	In-Plane Resolution, mm	Slice Distance, mm	Number of Slices	TE, ms	TR, ms
T <sub>1</sub> W 3D	3D	0.34 × 0.34	1.0	200	2.3	10
T <sub>1</sub> W AX	2D axial	0.65 × 0.65	2.5	65	18	637
T <sub>2</sub> W AX	2D axial	0.56 × 0.56	2.5	65	80	2924
FS T <sub>2</sub> W AX	2D axial	0.56 × 0.56	2.5	65	80	2924
T <sub>1</sub> W SAG	2D sagittal	0.56 × 0.56	2.5	35	18	523
T <sub>2</sub> W SAG	2D sagittal	0.37 × 0.37	2.5	35	80	2500
FS T <sub>2</sub> W SAG	2D sagittal	0.37 × 0.37	2.5	35	80	2500

Abbreviations: TE, echo time; TR, repetition time.

<sup>a</sup>Sequence names refer to T<sub>1</sub>-weighted 3D [T<sub>1</sub>W 3D], axial T<sub>1</sub>-w [T<sub>1</sub>W AX], axial T<sub>2</sub>-w [T<sub>2</sub>W AX], axial fat-suppressed T<sub>2</sub>-w [FS T<sub>2</sub>W AX], sagittal T<sub>1</sub>-w [T<sub>1</sub>W SAG], sagittal T<sub>2</sub>-w [T<sub>2</sub>W SAG], sagittal fat-suppressed T<sub>2</sub>-w MRI [FS T<sub>2</sub>W SAG].

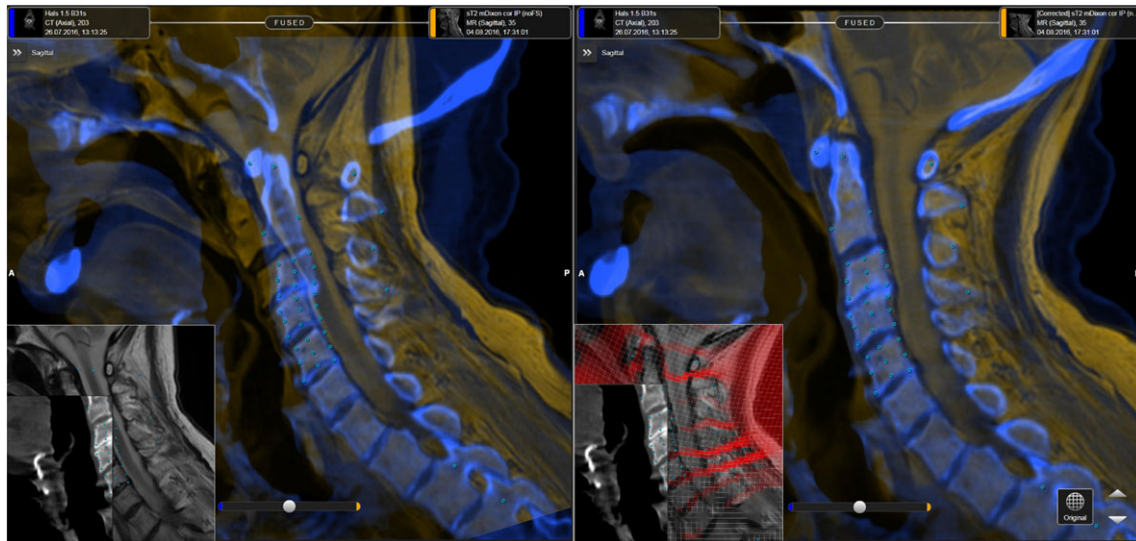


**FIGURE 1** Software visualization and graphical user interface of Elements Spine Curvature Correction (Image Fusion 3.0, Brainlab AG, Germany) basically, providing two image coregistration verification modes for superimposed datasets: the amber blue blending (large figures) and the spyglass tool (small figures), which both can be used to evaluate rigidly fused (left) and elastically deformed images (right). After elastic image fusion, all vertebrae show a high spatial correlation, which was achieved via nonrigid deformation of the intervertebral discs (indicated by the red color-coded deformation grid)

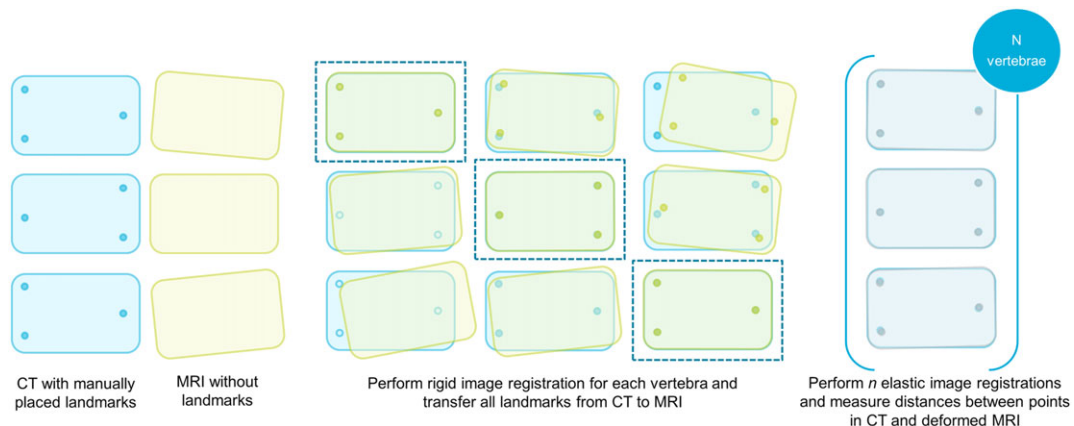


**FIGURE 2** Schematic illustration of the quantitative evaluation pathway based on anatomical landmarks, which are transferred from the reference (CT) image space to the target image space (MRI). Afterwards, the coordinates between rigidly and elastically landmarks are evaluated, ie, by determining their Euclidean distances, which quantifies by the target registration error (TRE) and provides assessment of the spatial correlation between the fused images after elastic image registration



in this study. Therefore, Euclidean distance measurements between rigidly and elastically fused anatomical landmarks were performed, where  $m$  landmarks related to bony anatomies were manually defined in the CT images (with  $m \gg n$ ) and afterwards—for each vertebra—separately transferred to each individual MRI scan by means of vertebra-specific ROI-based rigid fusions (Figure 2). Landmarks that correspond to the vertebra that served for the ROI-based fusion were tagged for reference accordingly. Landmarks related to other vertebrae were transferred as well and used to calculate  $n \times m$  target registration errors (TREs) by calculating the Euclidean distance between reference landmarks and rigidly ( $TRE_{\text{rigid}}$ ) or elastically transferred landmarks ( $TRE_{\text{elastic}}$ ). Thereby,  $n$  ROI-based rigid fusions were used as initial prealignment and thus as input for the elastic fusion algorithm. In total, 2204 elastic fusions were performed and evaluated in this study by using an automated postprocessing pipeline. Based on these data, the following analyses were performed:

(A) Artifact detection and data clustering based on descriptive  $TRE_{\text{elastic}}$  vs  $TRE_{\text{rigid}}$  analysis of individual fusion pairs.

(B) Box plot analysis of  $TRE_{\text{elastic}}$  as a function of the initial prealignment.

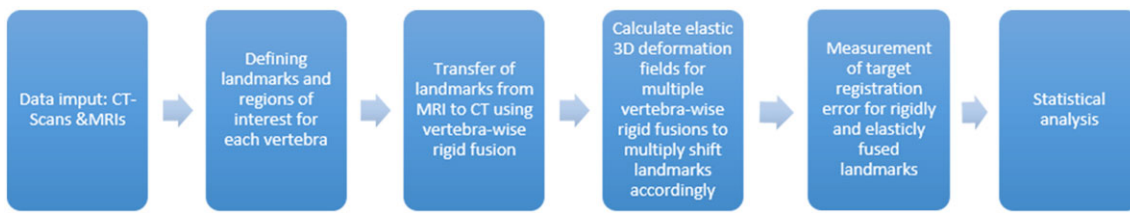
(C) Histogram analysis of  $TRE_{\text{elastic}}$  for different MRI contrasts and spatial sampling schemes.

Figure 3 provides a more visualized glance of the study procedure in a flowchart.

### 3 | RESULTS

The mean  $TRE_{\text{rigid}}$  value (averaged across subjects,  $n$  repetitions and  $m$  landmarks), eg, for 3D MRI data, was found to be 7.12 mm (median: 3.62 mm; Q95: 26.1 mm). Other MRI sequences showed similar values. Based on this data, different analyses were performed:

(A) First, in order to detect artifacts and cluster the data accordingly, the determined  $TRE_{\text{elastic}}$  values were plotted separately for different MRI sequences and head positions as a function of  $TRE_{\text{rigid}}$



**FIGURE 3** Study protocol presented as a flowchart

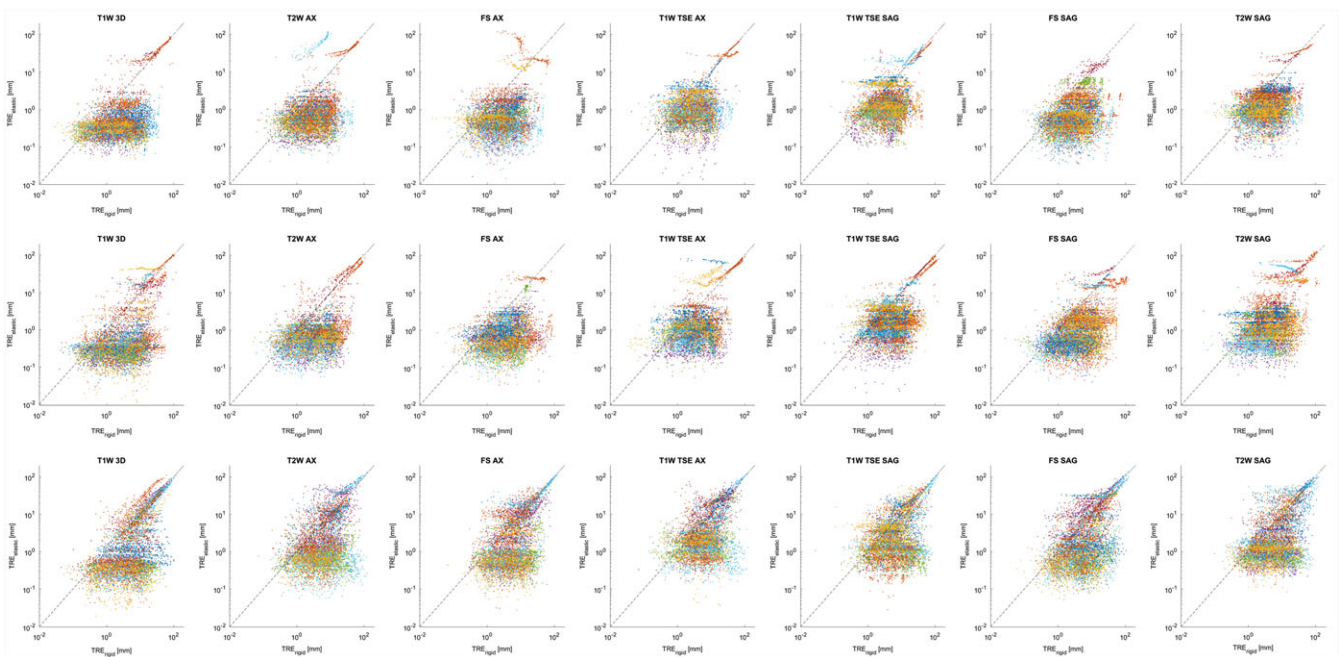


**FIGURE 4** Logarithmic plots of  $TRE_{\text{elastic}}$  as function of initial landmark displacement given by  $TRE_{\text{rigid}}$ . The color coding corresponds to different patients. Top, middle, and bottom row for each target image space refers to data acquired in neutral, flexed, and rotated head position, respectively

(Figure 4). It can be seen that a wide range of postural offsets was investigated (0–130 mm) with the highest  $TRE_{rigid}$  values for rotated head positions. After elastic fusion, the majority of landmarks are located below the line of identity (dashed line), which indicates a reduced mean Euclidian distance because of elastic image registration ( $TRE_{elastic} < TRE_{rigid}$ ). The  $TRE_{elastic}$  values are mainly distributed between 0 and 10 mm, while higher  $TRE_{elastic}$  values, such as above the line of identity, are mainly related to high  $TRE_{rigid}$  values and correspond to the same patient (same color coding). The latter indicates that registration artifacts are related to particular elastic fusions and thus to specific inputs.

(B) In order to investigate associations between the registration accuracy and specific inputs, such as defined by the initial prealignment and MR image properties (contrast, resolution, etc), mean  $TRE_{elastic}$  (averaged across  $m$  landmarks) were analyzed by using box plots for each MRI scan, with each as a function of the employed starting point (ie, vertebra used for prealignment). The results showed similar behavior across the examined MRI submodalities, with higher mean  $TRE_{elastic}$  values for prealignments using outermost vertebrae as an anatomical reference (Figure 5). In particular, atlas (corresponds to C0 at our study) and C1 as well as T3 and T4 as starting vertebra revealed higher susceptibility to image registration artifacts using the proposed method, eg, resulting in increased interquartile distances. Elastic image registration based on prealignment of centrally imaged vertebrae (C2–T2) provided mean image registration errors below 3 mm (below the red dashed line). In essence, the attached figures support the finding that the image registration accuracy is mainly independent of the preadjustment as long as none of the outermost vertebrae is chosen for the initial adjustment.

(C) To account for significant image artifacts, eg, because of inappropriate initial adjustments, an exclusion criterion was introduced, which allows excluding the corrupt results from further data analysis. Thereby, elastic image registrations such as based on the two

outermost vertebrae serving as starting vertebra and/or which showed a mean  $TRE_{elastic} > 2$  cm were excluded. It is presumed that the user intuitively performs manual prealignment based on centrally imaged vertebrae and detects obvious image registration artifacts (the latter was successfully verified by a survey of users), respectively. After applying this exclusion criterion, 1274 (of total = 2204) elastic fusions were considered for further analysis, while the mean  $TRE_{rigid}$  value for 3D MRI data decreased from 7.12 to 4.68 mm compared with nonfiltered data (as analyzed in sections A and B).

The results for filtered data are given in Table 2. It is shown that elastic image registration of cervical MRI and CT data is feasible with a median  $TRE_{elastic}$  below 1.34 mm considering 3D and 2D axial/sagittal MRI data, while fusion of  $T_1w$  3D MRI yields highest image registration accuracy with  $TRE_{elastic}$  values below 3.26 mm with 95% confidence. Elastic image registration of axial  $T_1w$ ,  $T_2w$ , and fat-suppressed  $T_2w$  MRI data generally yielded lower mean and median

**TABLE 2** Target registration error (TRE) for rigid and elastic fusion for different MRI protocols after application of the exclusion criterion

Sequence	Mean $TRE_{rigid}$ (SD)	Mean $TRE_{elastic}$ (SD)	Median $TRE_{elastic}$	95% Quantile $TRE_{elastic}$
$T_1w$ 3D	4.68 (6.15)	0.91 (2.55)	0.35	3.26
$T_1w$ AX	4.94 (5.78)	1.77 (2.85)	1.12	4.75
$T_2w$ AX	4.90 (6.09)	1.25 (2.43)	0.66	3.88
FS $T_2w$ AX	4.74 (5.43)	1.35 (2.56)	0.60	4.42
$T_1w$ SAG	6.16 (6.88)	2.23 (2.91)	1.34	6.02
$T_2w$ SAG	6.00 (7.50)	1.80 (2.98)	1.10	4.71
FS $T_2w$ SAG	5.30 (6.46)	1.49 (2.88)	0.66	5.11

All values given in millimeter. Exclusion criterion: exclusion of image registration results that were obtained based on the two outermost starting vertebrae and showing a mean registration of error  $> 2$  cm as described in the text.

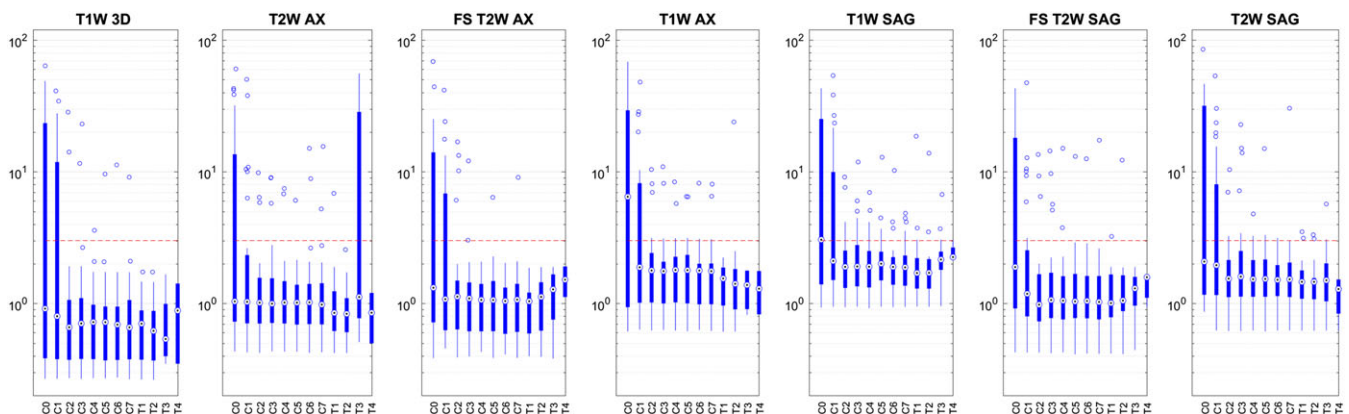


**FIGURE 5** Box plots of the mean target registration error (TRE values given in mm; using logarithmic y-axis scaling) as function of the starting vertebra. Using atlas (C0 corresponds to atlas) and C1 as well as T3 and T4 yields highest TRE values, while the other vertebrae typically reveal mean TREs below 3 mm (red dashed line)



TRE<sub>elastic</sub> values than the fusion of the correspondingly acquired sagittal MRI scans. Also, an impact of the MRI contrast can be seen, where for instance T<sub>1w</sub> 2D MRI shows lower image registration accuracy than T<sub>2w</sub> and fat-suppressed T<sub>2w</sub> MRI (for axial and sagittal sequences).

## 4 | DISCUSSION

The present study examines the image (co)registration accuracy of a novel semielastic image fusion method applied to retrospective cervical CT and MR image data clinically acquired in 10 patients while attempting to compensate for postural changes provoked by head flexion and head rotation within the MRI study. It has been shown that the proposed method provides reliable results with median TREs below 1.34 mm for different MRI protocols. Each individual rigid fusion for different head positions and each vertebra was evaluated and only highly accurate fusions were considered for further analysis. For this process, 3D T<sub>1w</sub> MRI data were used since it provides the highest spatial resolution and therefore allows the most reliable verification of the fusion. Accurate fusions were also applied to other MRI scans and evaluated afterwards anyway (to check for motion between the scans acquired during one particular head position).<sup>21,22</sup> In general, registration artifacts were primarily associated to specific input settings, such as when using outermost vertebrae (ie, atlas, C1, T3, and T4) as an anatomical reference for defining an initial (rigid) prealignment between the CT and MRI scan. This might be attributed to significant shifts of the spinal anatomies between both scans and to algorithmic constraints that limit the maximum translational and rotational compensation of rigidly morphed vertebrae and implies that the user needs to provide a good manual adjustment via the graphical user interface of the software prior to the elastic fusion calculation. Practically, as shown by initial analysis, user-defined initializations leading to significant elastic fusion errors of above 3 mm, on average (Figure 5), are mainly caused by severe registration artifacts with errors of above 1 cm, on average for individual fusion results. Such registration artifacts are principally clearly visible by the surgeon (as indicated by a survey of potential users) and thus might be discarded. Also, aligning outermost vertebrae is often associated with local lesions in these areas (ie, skull base or thoracic spine), where an elastic fusion of the entire cervical spine may not deem clinically necessary. Furthermore, and in concordance with other studies, higher registration accuracies were found for elastic fusion of 3D MRI data rather than using 2D MRIs, which might be explained by larger slice distances in 2D MRI and thus to higher (and more isotropic) spatial resolution in 3D MRI.<sup>3,20,23</sup> In addition, in this study, it was found that the registration accuracy of the proposed method is higher for axial than for sagittal MRI scans (Table 2). This might be related to higher slice coverage in axial scans and thus to incorporation of more extrapolated anatomical elements during the elastic fusion process of axial images compared with sagittal scans.<sup>3</sup> Nevertheless, mean TRE for 3D and 2D MRI sequences with mean target registration errors of 0.91 mm and below 2.23 mm for T<sub>1w</sub> 3D and 2D (sagittal) MRI data

are both below corresponding through-plan resolutions of 1 and 2.5 mm, respectively, which inherently limits the fusion accuracy as shown previously. For 2D MRI, however, the employed MRI contrast (T<sub>1</sub>- and T<sub>2</sub>-weighted as well as fat-suppressed MRI) showed a major effect on the image registration accuracy, where T<sub>1</sub>-weighting yielded the highest mean TRE for axial (1.77) and sagittal protocols (2.23 mm). T<sub>2</sub>-weighted fat and nonsuppressed protocols showed a mean TRE of 1.25 and 1.35 mm for axial and 1.80 and 1.49 mm for sagittal MRI data. The highest TREs for T<sub>1</sub>-weighted are potentially related to lower image contrast between vertebra and intervertebral discs in T<sub>1w</sub> MRI than in T<sub>2w</sub> MRI. Nevertheless, the reported values in this study indicate higher fusion accuracy than typically observed previously.<sup>24-26</sup>

In order to evaluate the registration accuracy of the proposed method, a MI-based rigid image registration functionality served as reference, which was used to separately transfer landmarks for each vertebrae from the CT image space to the different MRI paces (using the segmented vertebra volume to define a cubic ROI in the CT space in which the fusion is performed). Thereby, manual determination of identical anatomic landmarks and therefore the imminent irreproducibility of the results were avoided in this study. Another limitation of this study might be related to bulk motion artifacts in MRI intrinsically reducing the image and thus coregistration quality. In this study—although an extensive MRI protocol was applied—no significant motion-induced artifacts occurred in the MRI data.<sup>27</sup>

The radiologic evaluations of the patients with scoliosis pose serious challenges because of some substantial differences; for instance, the CT often has to be taken in standing position that makes the patient more prone to unwanted movements that could introduce significant obstacles to image registration.<sup>28</sup> The body of the literature on the application of image registration for spinal surgery is not comparable with those concerning other fields of medicine, and they have been performed on cadavers, which, regarding the different and more feasible workflow of the imaging and assessment process, might not be completely generalizable and applicable when dealt with patients, yet many of these studies yield greater errors than that of achieved by the present study.<sup>29</sup>

In summary, this work thoroughly examines image registration accuracy of a novel semielastic image coregistration method by assessing cervical CT and MRI data obtained in a representative cohort of patients. Thereby, reliable results were shown with mean target registration errors below 0.91 and 2.23 mm for 3D and 2D MRI data, respectively. Since the cervical spine is the most flexible part of the spine, and thus shows the highest translational and rotational displacements of the vertebrae relative to each other, this experimental setup provides comprehensive assessment of the method, which is thought to compensate for postural changes in multimodal and follow-up imaging studies. Future studies are required in order to determine the image registration accuracy in other parts of the spine and soft tissue anatomies, as well as for alternate clinical indications and varying MRI protocols.

## FUNDING

The study was financially supported by Brainlab AG, Germany.

## CONFLICT OF INTEREST

None of the authors, who are not full-time employees at Brainlab (ie, P.H. and J.K.), directly received any money from Brainlab. Financial compensation was only provided for acquisition, anonymization, and transfer of medical image data (defined by contract). At any time, the authors had the scientific freedom to contribute to study design and data analysis in an independent manner. Further, it was always pursued to work in accordance with the principles of good manufacturing practice.

## ORCID

Ashkan Rashad  <https://orcid.org/0000-0003-3743-8658>

## REFERENCES

- Crum WR, Hartkens T, Hill DL. Non-rigid image registration: theory and practice. *Br J Radiol*. 2004;77 Spec No 2(suppl\_2):S140-S153.
- Benamer S, Mignotte M, Parent S, Labelle H, Skalli W, de Guise J. 3D/2D registration and segmentation of scoliotic vertebrae using statistical models. *Comput Med Imaging Graph: the official journal of the Computerized Medical Imaging Society*. 2003;27(5):321-337.
- Nemec SF, Donat MA, Mehraïn S, et al. CT-MR image data fusion for computer assisted navigated neurosurgery of temporal bone tumors. *Eur J Radiol*. 2007;62(2):192-198.
- Van den Elsen PA, Pol E-J, Viergever MA. Medical image matching-a review with classification. *IEEE Eng Med Biol Mag*. 1993;12(1):26-39.
- Brown LG. A survey of image registration techniques. *ACM Computing Surveys (CSUR)*. 1992;24(4):325-376.
- Tomazevic D, Likar B, Slivnik T, Pernus F. 3-D/2-D registration of CT and MR to X-ray images. *IEEE Trans Med Imaging*. 2003;22(11):1407-1416.
- Sure U, Alberti O, Petermeyer M, Becker R, Bertalanffy H. Advanced image-guided skull base surgery. *Surg Neurol*. 2000;53(6):563-572.
- Thompson PM, Woods RP, Mega MS, Toga AW. Mathematical/computational challenges in creating deformable and probabilistic atlases of the human brain. *Hum Brain Mapp*. 2000;9(2):81-92.
- Toga AW, Thompson PM. The role of image registration in brain mapping. *Image Vis Comput*. 2001;19(1):3-24.
- Meijering EH, Niessen WJ, Viergever M. Retrospective motion correction in digital subtraction angiography: a review. *IEEE Trans Med Imaging*. 1999;18(1):2-21.
- Rosenman JG, Miller EP, Tracton G, Cullip TJ. Image registration: an essential part of radiation therapy treatment planning. *Int J Radiat Oncol Biol Phys*. 1998;40(1):197-205.
- Hutton BF, Braun M, Thurffjell L, Lau DY. Image registration: an essential tool for nuclear medicine. *Eur J Nucl Med Mol Imaging*. 2002;29(4):559-577.
- Makela T, Clarysse P, Sipila O, et al. A review of cardiac image registration methods. *IEEE Trans Med Imaging*. 2002;21(9):1011-1021.
- Song G, Han J, Zhao Y, Wang Z, Du H. A review on medical image registration as an optimization problem. *Curr Med Imaging Rev*. 2017;13(3):274-283.
- Razlighi QR, Kehtarnavaz N, Yousefi S. Evaluating similarity measures for brain image registration. *J Vis Commun Image Represent*. 2013;24(7):977-987.
- Gaens T, Maes F, Vandermeulen D, Suetens P, editors. Non-rigid multimodal image registration using mutual information. International Conference on Medical Image Computing and Computer-Assisted Intervention; 1998: Springer.
- Ireland RH, Dyker KE, Barber DC, et al. Nonrigid image registration for head and neck cancer radiotherapy treatment planning with PET/CT. *Int J Radiat Oncol Biol Phys*. 2007;68(3):952-957.
- Lavallée S, Sautot P, Troccaz J, Cinquin P, Merloz P. Computer-assisted spine surgery: a technique for accurate transpedicular screw fixation using CT data and a 3-D optical localizer. *J Image Guid Surg*. 1995;1(1):65-73.
- Kaminsky J, Rodt T, Zajaczek J, Donnerstag F, Zumkeller M. Mehrsegmentale Bildfusion an der Wirbelsäule/multisegmental image fusion of the spine. *Biomed Tech (Berl)*. 2004;49(3):49-55.
- Klabbers BM, de Munck JC, Slotman BJ, et al. Matching PET and CT scans of the head and neck area: development of method and validation. *Med Phys*. 2002;29(10):2230-2238.
- Karnik VV, Fenster A, Bax J, et al. Assessment of image registration accuracy in three-dimensional transrectal ultrasound guided prostate biopsy. *Med Phys*. 2010;37(2):802-813.
- van de Ven WJ, Hu Y, Barentsz JO, Karssemeijer N, Barratt D, Huisman HJ. Biomechanical modeling constrained surface-based image registration for prostate MR guided TRUS biopsy. *Med Phys*. 2015;42(5):2470-2481.
- Casselmann JW, Kuhweide R, Deimling M, Ampe W, Dehaene I, Meeus L. Constructive interference in steady state-3DFT MR imaging of the inner ear and cerebellopontine angle. *AJNR Am J Neuroradiol*. 1993;14(1):47-57.
- Harmouche R, Cheriet F, Labelle H, Dansereau J. 3D registration of MR and X-ray spine images using an articulated model. *Comput Med Imaging Graph: the official journal of the Computerized Medical Imaging Society*. 2012;36(5):410-418.
- Daisne JF, Blumhofer A. Atlas-based automatic segmentation of head and neck organs at risk and nodal target volumes: a clinical validation. *Radiat Oncol (London, England)*. 2013;8(1):154.
- Doody MM, Lonstein JE, Stovall M, Hacker DG, Luckyanov N, Land CE. Breast cancer mortality after diagnostic radiography: findings from the U.S. Scoliosis Cohort Study. *Spine (Phila Pa 1976)*. 2000;25(16):2052-2063.
- Nemec SF, Peloschek P, Schmook MT, et al. CT-MR image data fusion for computer-assisted navigated surgery of orbital tumors. *Eur J Radiol*. 2010;73(2):224-229.
- Bamba Y, Nonaka M, Nakajima S, Yamasaki M. Three-dimensional reconstructed computed tomography-magnetic resonance fusion image-based preoperative planning for surgical procedures for spinal lipoma or tethered spinal cord after myelomeningocele repair. *Neurol Med Chir*. 2011;51(5):397-402.
- Sumanaweera T, Glover G, Song S, Adler J, Napel S. Quantifying MRI geometric distortion in tissue. *Magn Reson Med*. 1994;31(1):40-47.

**How to cite this article:** Rashad A, Heiland M, Hiepe P, et al. Evaluation of a novel elastic registration algorithm for spinal imaging data: A pilot clinical study. *Int J Med Robotics Comput Assist Surg*. 2019;15:e1991. <https://doi.org/10.1002/rcs.1991>